

A Novel Tunable Fiber-Optic Microwave Filter Using Multimode DCF

Kwang-Hyun Lee, Woo-Young Choi, *Member, IEEE*, S. Choi, and K. Oh

Abstract—We demonstrate a novel tapped delay-line fiber-optic microwave filter composed of four-mode dispersion compensation fiber (DCF) and a light source. The optical delay line is realized by the DCF guided modes having different velocities. The free-spectral range of the filter can be controlled by tuning the incident light wavelength.

Index Terms—Fiber-optic microwave filter, multimode dispersion compensation fiber (DCF), optical delay line.

I. INTRODUCTION

OPTICAL DELAY lines are attracting the interest of many research groups due to their advantages in microwave signal processing applications such as wide bandwidth, wide dynamic range, and low loss. Owing to these advantages, optical delay lines find applications for photonic analog-to-digital converters [1], optically controlled phased-array antennas [2], and fiber-optic microwave filters [3]–[5].

Recently, several different methods have been demonstrated to realize the fiber-optic microwave filter using optical delay lines. In these methods, the optical delay lines are produced with tunable optical sources and high dispersive fibers (HDFs) having different lengths or a chirped fiber Bragg grating. However, these methods have the limitation that, in order to increase the tap number, the number of optical sources or HDF has to be increased.

In this letter, we propose and demonstrate a novel fiber-optic microwave filter composed of one optical source and one multimode dispersion compensation fiber (DCF). The proposed filter uses the velocity difference among guided modes in multimode DCF as the basic mechanism for optical delay lines and the power coupling ratio into these modes is controlled by the hollow optical fiber (HOF) [6]. In this filter, the tap number is determined by the mode number in DCF, thus multitaps can be achieved with one multimode DCF. In addition, the free-spectral range (FSR) can be easily controlled by tuning the incident light wavelength.

II. THEORY AND SIMULATION RESULTS

The structure for the proposed filter is shown in Fig. 1. The filter consists of a broad-band source, a modulator, an optical-

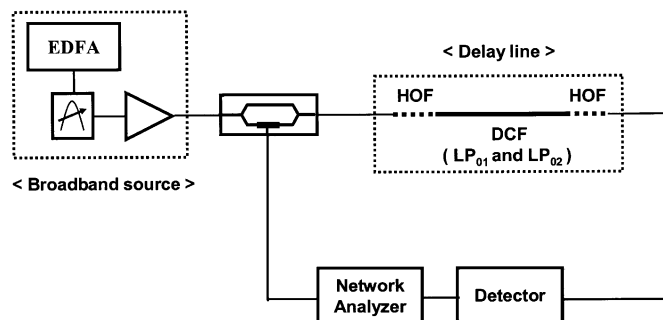


Fig. 1. Configuration and measurement setup for the proposed filter.

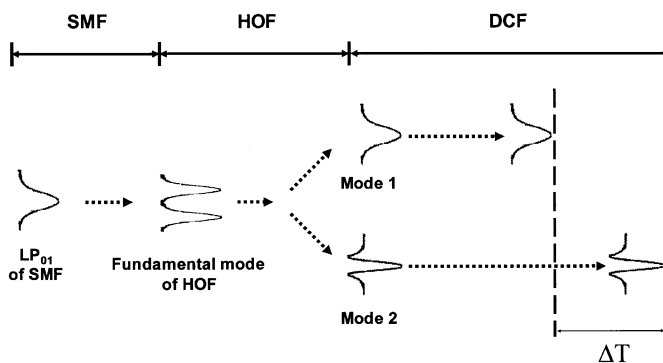


Fig. 2. Schematics for field propagation within optical-delay-line device.

delay-line device made up of multimode DCF and HOF, and a photodetector (PD). In Fig. 2, the field propagation within the optical-delay-line device is schematically shown. As shown in the figure, the fundamental mode (LP_{01}) of single-mode fiber (SMF) is first coupled into the ring-shaped mode in HOF, which is in turn coupled into DCF modes. The HOF is used between SMF and DCF in order to control the coupling ratio from SMF LP_{01} mode into DCF modes, because, without HOF, most LP_{01} power is coupled into DCF LP_{01} mode. The coupling ratio can be controlled by changing the size of HOF hole radius [7]. The exited modes have different velocities within DCF, causing the time-delay difference at the end of DCF.

For our first demonstration, the DCF is designed to guide four modes, LP_{01} , LP_{11} , LP_{21} , and LP_{02} . Among these modes, only LP_{01} and LP_{02} modes are excited in DCF, because coupling from the HOF fundamental mode to DCF LP_{11} and LP_{21} modes is not allowed due to the mode orthogonality [7]. The amount of the time-delay difference between LP_{01} and LP_{02} modes can be expressed as

$$\Delta T = \left(\frac{d}{d\omega}(\beta_{01}) - \frac{d}{d\omega}(\beta_{02}) \right) L = (n_{g,01} - n_{g,02}) \frac{L}{c} \quad (1)$$

Manuscript received December 9, 2002; revised March 11, 2003. This work was supported by the Ministry of Science and Technology of Korea through the National Laboratory Program.

K.-H. Lee and W.-Y. Choi are with the Department of Electrical and Electronic Engineering, Yonsei University, Seoul 120-749, Korea (e-mail: wchoi@yonsei.ac.kr).

S. Choi and K. Oh are with the Department of Information and Communications, Kwangju Institute of Science and Technology (K-JIST), Kwangju, Korea. Digital Object Identifier 10.1109/LPT.2003.813451

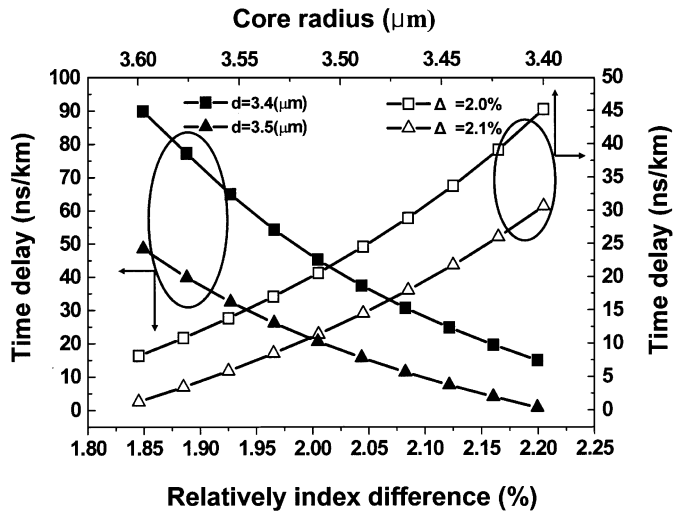


Fig. 3. Calculated results of the time-delay difference within DCF as a function of the relative index difference (Δ), core radius (d) at fixed wavelength (1530 nm).

where β_{0i} is the propagation constant for the LP_{0i} mode, $n_{g,0i}$ is the group index for the LP_{0i} mode, c is the light velocity, and L is the DCF length. This time-delay difference is dependent on the source wavelength and the waveguide structure of DCF such as core radius (d) and relative index difference between core and cladding ($\Delta = (n_1 - n_2)/n_2$, where n_1 is core index and n_2 is cladding index).

To calculate the time-delay difference, the group indexes of LP_{01} and LP_{02} modes are obtained by solving the wave equation in DCF [8]. The calculated results are shown in Figs. 3 and 4. Fig. 3 shows the time-delay difference as a function of Δ and d at a fixed wavelength of 1530 nm. Fig. 4(a) shows the time-delay difference as a function of the source wavelength and Δ at a fixed value of $d = 3.5 \mu\text{m}$ and Fig. 4(b) shows the time-delay difference as a function of the source wavelength and d at fixed value of $\Delta = 2.0\%$. It is clearly shown that the time-delay difference is continuously tunable. The time-delay difference increases as the source wavelength increases. However, this trend strongly depends on the fiber structure, and it is possible for the time-delay difference to decrease as the wavelength increases for different fiber structures, as is the case in [9].

From the calculated results, proper values of core radius and relative index difference can be determined to obtain desired amount of the time-delay difference.

The two modes are added incoherently and detected by the PD. If the two modes have equal power, the detected optical power (P_{opt}) at the modulation frequency can be expressed as

$$P_{\text{opt}} \propto \left| \cos \left(\frac{\beta'_{01}L - \beta'_{02}L}{2} \cdot \omega_c \right) \right| = \left| \cos \left(\frac{\Delta T}{2} \omega_c \right) \right| \quad (2)$$

where ω_c is the modulation frequency, β'_{0i} is the first-order derivative of the propagation constant for LP_{0i} mode, and L is the DCF length. The equation shows that the detected optical power depends on the time-delay difference (ΔT).

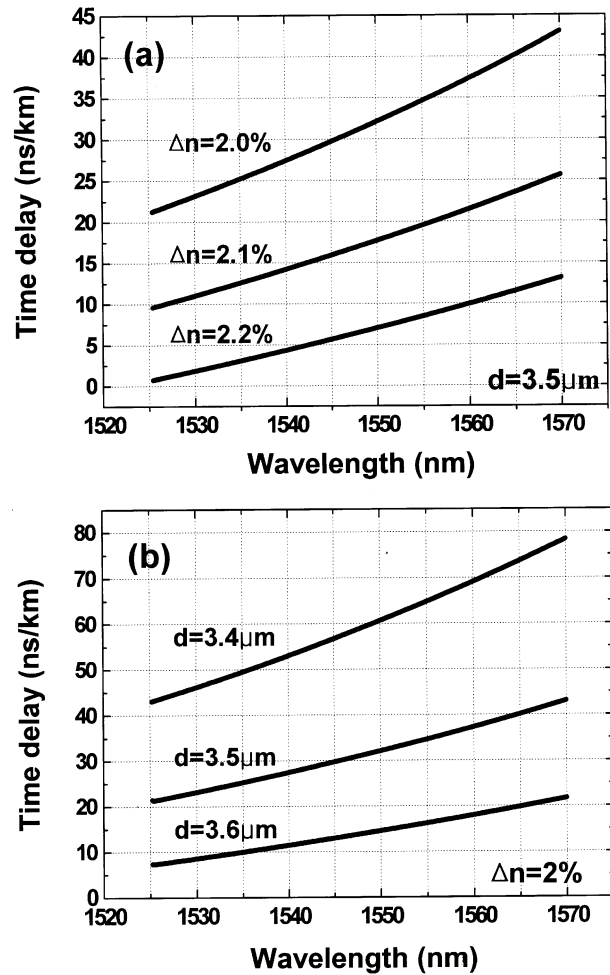


Fig. 4. Calculated results of the time-delay difference within DCF as a function of (a) the source wavelength and relative index difference at fixed core radius ($3.5 \mu\text{m}$) and (b) the source wavelength and core radius at fixed relative index difference (2.0%).

III. EXPERIMENT AND RESULTS

Fig. 1 shows the experimental setup for demonstrating a two-tap filter with two DCF modes, LP_{01} and LP_{02} . As shown in the figure, the broad-band source consists of an erbium-doped fiber amplifier (EDFA) and a tunable filter. The output signal of the broad-band source is produced by filtering the EDFA amplified spontaneous emission with the tunable filter having 0.4-nm bandwidth, and consequently, the coherence problem is eliminated [10]. This optical signal is modulated by the radio-frequency signal of the network analyzer (NA) and the modulated signal enters the optical-delay-line device. At the end of 46-m-long DCF, the two DCF modes (LP_{01} and LP_{02}) are converted back to the fundamental mode (LP_{01}) of SMF by HOF and detected by PD. This additional conversion from DCF to HOF to SMF is necessary because the PD used in our experiment is pigtailed with SMF. The HOF used in the experiment has the hole radius of $1 \mu\text{m}$, which is larger than the optimal value of $0.6 \mu\text{m}$, in order to achieve a 50:50 coupling ratio for LP_{01} and LP_{02} modes. In the present investigation for feasibility, we achieved the 50:50 coupling ratio by actively aligning the HOF to DCF so that their center axes are slightly off. This active alignment should not be necessary with a properly designed HOF which can be easily fusion-spliced to DCF.

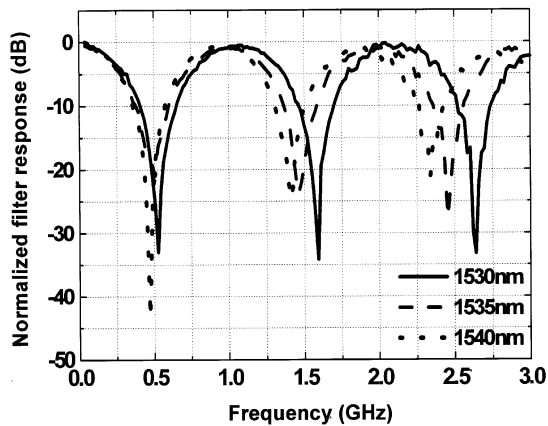


Fig. 5. Measured frequency response of the proposed filter with two taps. (DCF length = 46 m).

Fig. 5 shows the results of NA measurement for the modulation frequency ranging from 40 MHz to 3 GHz. The measured FSR is 1.0659 GHz at source wavelength of 1530 nm, and the time-delay difference is about 0.9817 ns (20.395 ns/km). At the source wavelength of 1535 nm, the FSR is 0.9537 GHz (22.79 ns/km) and at 1540 nm, the FSR is 0.9350 GHz (23.25 ns/km). The tuning characteristic of FSR is shown clearly with the estimated tuning rate of 0.285 ns/km · nm. In addition, the notch rejection is more than 20 dB for wavelengths covered in the experiment. Comparing these results with the simulation results, it can be estimated that the DCF core radius is 3.58 μm and the relative index difference is 1.93%.

IV. CONCLUSION

In this letter, we have proposed and demonstrated a novel tunable fiber-optic microwave filter with two taps using just one

short DCF having LP_{01} , LP_{02} modes and one tunable source. In the filter, the FSR can be easily and continuously tuned by changing the source wavelength. Moreover, if the DCF is designed to have additional modes, LP_{0m} or HOF is designed to allow coupling into LP_{11} , LP_{21} DCF modes, it is possible to make fiber-optic microwave filters having multiple taps without additional sources or fibers.

REFERENCES

- [1] F. Coppinger, A. S. Bhushan, and B. Jalali, "12 Gsample/s wavelength division sampling analogue-to-digital converter," *Electron. Lett.*, vol. 36, no. 4, pp. 316–317, 2000.
- [2] I. Frigyes and A. J. Seeds, "Optically generated true-time delay in phased-array antennas," *IEEE Trans. Microwave Theory Tech.*, vol. 43, pp. 2378–2386, Sept. 1995.
- [3] M. Y. Frankel and R. D. Esman, "Fiber-optic tunable microwave transversal filter," *IEEE Photon. Technol. Lett.*, vol. 7, pp. 191–193, Feb. 1995.
- [4] D. Norton, S. Johns, and R. Soref, "Tunable microwave filtering using high dispersion fiber time delays," *IEEE Photon. Technol. Lett.*, vol. 6, pp. 831–832, July 1994.
- [5] J. Capmany, D. Pastor, and B. Ortega, "New and flexible fiber-optic delay-line filters using chirped bragg gratings and laser arrays," *IEEE Trans. Microwave Theory Tech.*, vol. 47, pp. 1321–1326, July 1999.
- [6] S. Choi, K. Oh, W. Shin, and U. C. Ryu, "Low loss mode converter based on adiabatically tapered hollow optical fiber," *Electron. Lett.*, vol. 37, no. 13, pp. 823–825, 2001.
- [7] S. Choi, W. Shin, and K. Oh, "Higher-order-mode dispersion compensation technique based on mode converter using hollow optical fiber," in *Tech. Dig. Conf. Optical Fiber Communication*, 2002, Paper WA6.
- [8] C. D. Poole, J. M. Wiesenfeld, D. J. Digiovanni, and A. M. Vengsarkar, "Optical fiber-based dispersion compensation using higher order modes near cutoff," *J. Lightwave Technol.*, vol. 12, pp. 174–1758, Oct. 1994.
- [9] D. Menashe, M. Tur, and Y. Danziger, "Interferometric technique for measuring of high order modes in optical fibers," *Electron. Lett.*, vol. 37, no. 24, pp. 1439–1440, 2001.
- [10] A. H. Quoc and S. Tedjini, "Experimental investigation on the optical unbalanced Mach–Zehnder interferometers as microwave filters," *IEEE Microwave Guided Wave Lett.*, vol. 4, pp. 183–185, June 1994.